a.i. solutions®

Examining the Feasibility of Relative-Only Navigation for Crewed Missions to Near Rectilinear Halo Orbits

Written by: Michael J. Volle, Diane C. Davis

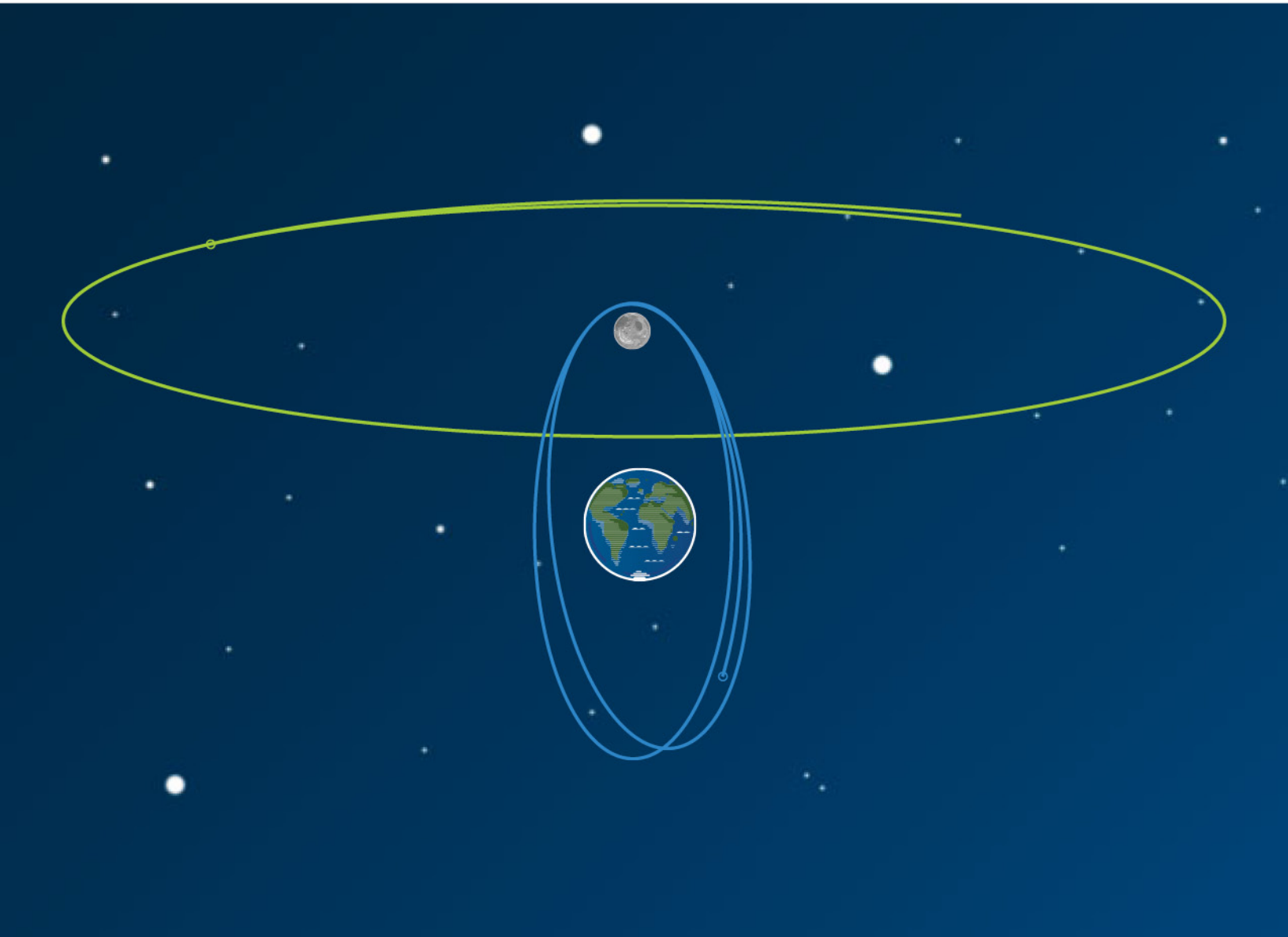

AAS 18-351

EXAMINING THE FEASIBILITY OF RELATIVE-ONLY NAVIGATION FOR CREWED MISSIONS TO NEAR RECTILINEAR HALO ORBITS

Michael J. Volle* **and Diane C. Davis†**

Recently, lunar Near Rectilinear Halo Orbits (NRHO) have been the focus of much study, and they have been selected as the target orbit for the Gateway mission, formerly the Deep Space Gateway. Also, the Deep Space Network (DSN) is increasingly congested and over-subscribed. In this work, the performance of relative-only navigation between a spacecraft in an NRHO and a relay in a Distant Retrograde Orbit is examined and compared to simulated DSN tracking using a Square Root Information Filter. Various tracking scenarios are examined using a closed-loop simulation where navigation errors inform maneuver planning and maneuver execution errors affect navigation performance. Results indicate that relative-only navigation can provide comparable levels of orbit determination error and orbit maintenance costs.

INTRODUCTION

Lunar Near Rectilinear Halo Orbits (NRHOs) are currently the primary candidate for the target orbit for the Gateway mission, formerly known as the Deep Space Gateway.[1,2] The NRHO orbit class is selected because it exhibits several useful advantages for human spaceflight.[3] These include low orbit maintenance costs, low orbit insertion costs, low orbit transfer costs, and resonant periods that minimize shadowing and communications blockages. Each of these characteristics has been examined in previous works.[3–5]

Construction and usage of the Gateway, a maneuverable, habitable lunar-orbit staging vehicle for deep space missions, will occur over multiple missions and will contain phases of crewed activity and uncrewed, quiescent operations.[6,7] As such, any orbit maintenance or navigation analysis should incorporate the dynamical disturbances associated with both phases. The uncrewed phase will generally be more quiescent than the crewed phases, as the main orbit disturbances will be momentum unload and orbit maintenance maneuvers (OMM). However during crewed phases, more orbit disturbances are introduced by the added impacts of human activity. These disturbances are events like CO_2 and waste dumps, additional momentum unloads, and attitude slews. These disturbances can be frequent and unplanned, and occur at varying time intervals, making them potentially difficult to model for navigation.

Typically, missions such as Gateway rely on the Deep Space Network (DSN) for tracking; however as of 2015, the DSN supported about 40 deep-space missions and was routinely oversubscribed by about 30%. This demand translates to about 500 hours of over-subscription per week, roughly

*Principal Systems Engineer, a.i. solutions, Inc., 4500 Forbes Blvd. Ste. 300, Lanham, MD 20706, michael.volle@ai-solutions.com

†Principal Systems Engineer, a.i. solutions, Inc., 2224 Bay Area Blvd. Ste. 415, Houston, TX 77058, diane.davis@ai-solutions.com

equivalent to the work of 4 additional antennas.[8] Furthermore, there are currently 6 more missions to Mars (comprising 9 spacecraft) planned for the 2020 launch window, creating an unprecedented level of demand.[9] In an attempt to alleviate the expected congestion, the DSN has implemented the Multiple Spacecraft Per Antenna (MSPA) technique, allowing for shared antenna time. However this is restricted to spacecraft within the same beam-width and all secondary spacecraft are limited to downlink only.[10]

Given this over-subscription, it makes sense to investigate alternative navigation strategies that might alleviate these scheduling constraints. Relative navigation approaches in cis-lunar space have been investigated previously, and they have demonstrated suitable navigation accuracies for robotic missions.[11–13] In addition, NASA has contracted for additional studies on technologies related to peer-to-peer navigation in cis-lunar space.[14] The previous works typically considered the combination of low-lunar orbit and Halo obits for the relative navigation scenario. This analysis considers relative navigation between an NRHO and a DRO.

The orbit chosen for the Gateway is an L2 Southern NRHO with an average periapsis altitude of approximately 1800 km, an apoapsis altitude of 68,000 km, and a period of about 6.5 days. This orbit exhibits a 9:2 resonance with the Moon's synodic orbit.[4] For this analysis, the specific orbit chosen for the navigation relay is a Distant Retrograde Orbit (DRO) with an average altitude of 75,000 km and a period of about 13 days (but is not in resonance with the NRHO). The orbits appear in Figure 1, as viewed in the rotating system from the Earth-Moon line, below the plane of the Moon's orbit.

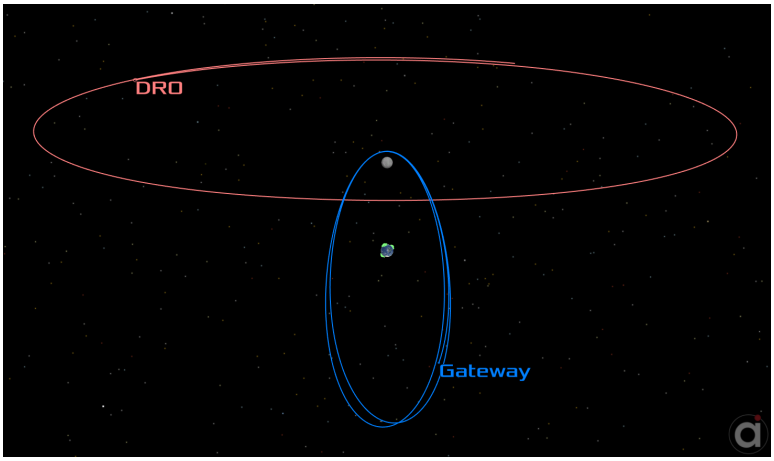

Figure 1: NRHO and DRO Orbit Geometry

The DRO is selected as the relay orbit because it provides at least one distinct advantage for alleviating the burden on the DSN. The stability of the orbit allows for (almost) no OMMs.[15,16] With no OMMs and an autonomous relative navigation strategy, ground based tracking and telemetry can be minimized to vehicle state-of-health information. These telemetry links can be provided by alternatives to the DSN, such as the Universal Space Network (USN).

The 9:2 resonant NRHO - DRO orbit pairing does not preclude line-of-sight blockages by the Moon. However, the resonant nature of the NRHO does help to provide stable, predictable behavior in this regard. Over the course of one year, the pairing goes through three different "eclipse" seasons of blockages between the two spacecraft. From the geometry, the lunar blockages only occur when

the DRO is near its maximum Y-amplitude (in rotating coordinates) and the NRHO is near the opposite ascending/descending node. Due to the elongation of the NRHO, a spacecraft moves quickly through the plane of the DRO. This means that each blockage is relatively short in duration, typically an hour or so. In total, the amount of blockage time is minimal, totaling only about 14 hours per year. See Figure 2 for a plot of the accumulated blockage time over the course of one year. This analysis covers the time period that incorporates the first set of blockages in the March/April time-frame.

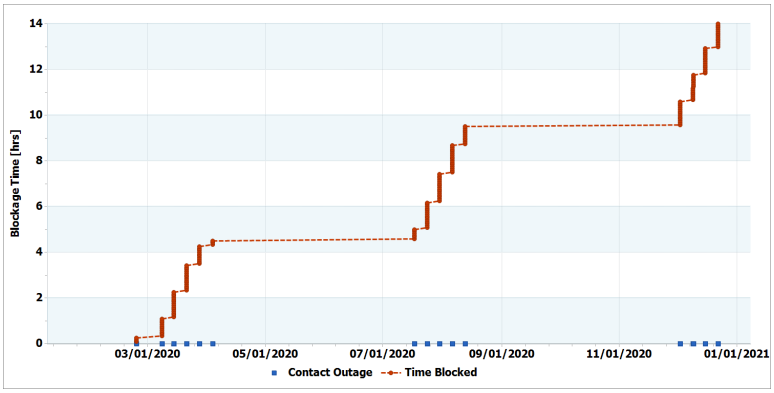

Figure 2: Cumulative NRHO and DRO Contact Outages Over One Year

For Gateway, one method of orbit maintenance under study is a receding-horizon approach for x-axis crossing control.[5,17] Initially, a periodic NRHO in the Circular Restricted Three Body model is used to target a quasi-periodic NRHO in a higher-fidelity ephemeris force model. The resulting quasi-periodic orbits have been extended up to 15 years in duration, and are used as a source of targeting conditions for orbit maintenance maneuvers (OMMs). The receding-horizon approach then targets the reference Rotating Libration Point (RLP) frame x-velocity at periapsis multiple revolutions ahead of the maneuver planning state. These reference trajectories have been generated under both uncrewed and crewed orbital conditions.[4]

Previous works examining orbit maintenance costs for NRHOs have only used notional (static) navigation errors as part of the maneuver planning process, or have been based on linear covariance analysis.[4] To perform a more detailed navigation analysis, a closed-loop simulation is developed that incorporates both realistic navigation errors and maneuver execution errors associated with the receding-horizon orbit maintenance approach. Navigation solutions are computed using simulated tracking data that is processed through a Square-Root Information Filter (SRIF).[18,19] At apoapsis, the receding-horizon approach is used to plan OMMs using the navigation state. Maneuver execution errors are then applied to the truth simulation, while the SRIF is only allowed knowledge of the planned maneuver. This approach allows for navigation errors to realistically affect maneuver planning, and for maneuver execution errors to affect navigation accuracy.

DYNAMICAL MODELS

The baseline dynamical model shared across all propagations in the simulation is outlined in Tables 1 and 2. The configuration of the spacecraft in the NRHO is chosen to approximate the Orion spacecraft both in terms of mass and disturbances. The orbit disturbances associated with crewed activity are also listed, as determined by a previous analysis of the Orion vehicle.[20] All orbit disturbances and OMMs are applied impulsively. These disturbances include attitude slews

and deadbands, as well as CO_2 and wastewater dumps (venting) to expel crew waste. The torques caused by these perturbations lead to more frequent momentum desaturations. Slews to OMM attitude are assumed to be performed by the Reaction Control System (RCS) thrusters to reduce time away from nominal crewed attitude. The slews produce additional translational errors. As a result of the added perturbations, OMMs are generally required every revolution during crewed operations, and the OMM ΔV magnitudes are higher. The additional disturbances resulting from crew presence at the Gateway lead to degraded Orbit Determination (OD) accuracy unless additional ground or relative tracking observations are available.

Table 1: NRHO Propagation Models

	Simulation	Filter
Planetary Ephemeris	DE 430	DE 430
Point Mass Gravity	Sun, Mercury, Venus, Earth, Mars, Jupiter, Saturn, Uranus, Neptune	Sun, Mercury, Venus, Earth, Mars, Jupiter, Saturn, Uranus, Neptune
Lunar Gravity Field	30x30	30x30
Solar Radiation Pressure	spherical 24000 kg, 80 m^2 Cr = 2.0	spherical 24000 kg, 80 m^2 Cr = 2.0 $\pm 3\sigma$
Orbit Maintenance	Planned $\pm$ 1% mag / 1 deg (3σ)	Planned only
CO_2 Dumps	0.08348 cm/s every 10 min Random Direction	–
Attitude Slews	0.06975 cm/s every 190 min Random Direction	–
Waste Dumps	0.18840 cm/s every 180 min Random Direction	–
Attitude DeadBands	0.002004 cm/s every 70 min Random Direction	–

Table 2: DRO Propagation Models

	Simulation	Filter
Planetary Ephemeris	DE 430	DE 430
Point Mass Gravity	Sun, Mercury, Venus, Earth, Mars, Jupiter, Saturn, Uranus, Neptune	Sun, Mercury, Venus, Earth, Mars, Jupiter, Saturn, Uranus, Neptune
Lunar Gravity Field	30x30	30x30
Solar Radiation Pressure	spherical 2000 kg, 30 m^2 Cr = 1.5	spherical 2000 kg, 30 m^2 Cr = 1.5 $\pm 3\sigma$

The orbit maintenance strategy implemented in the current analysis is an x-axis crossing control algorithm. This stationkeeping method employs a pre-computed long-horizon reference trajectory as a target. Periodic OMMs target components of the reference trajectory to ensure the spacecraft remains near the desired orbit. In the current implementation, the OMMs occur at apoapsis. The

target is a single component of the reference trajectory, the x-component of rotating velocity in the Earth-Moon rotating frame, V_x, along a receding horizon. A differential corrector is employed to compute the ΔV needed at apoapsis to achieve the reference value of V_x at periapsis 6.5 revolutions (about 42 days) downstream. If the targeter fails to converge, the horizon is reduced until convergence is achieved. The computed maneuver is performed only if the ΔV magnitude is above a minimum threshold. For this analysis, the minimum threshold is set to 0.15 cm/s. The spacecraft is then propagated to the subsequent apoapsis, and the process is repeated, allowing an OMM once per revolution. Further details appear in Guzzetti et al.[5]

NAVIGATION MODEL

As stated previously, all orbit solutions are estimated using a SRIF. The SRIF matches the algorithms that are planned as part of Orion ground navigation tools.[19] For this analysis, there are two filter configurations: a configuration that estimates the NRHO spacecraft state based on DSN measurements (referred to as DSN-solutions or DSN-based) and a configuration that estimates the NRHO state based on the relative measurements from the DRO relay (referred to as DRO-solutions or DRO-based). The DSN-based solutions are intended as a baseline comparison for the DRO-based results. The details of these configurations are captured in the following section.

Filter Estimation States

For the DRO-based solutions, two options exist for how to handle the state of the navigation satellite in the DRO:

1. Rely on only the relative measurements in the simulation, which then requires that the DRO state be added to the NRHO filter state.

2. Rely on ground-based measurements for the DRO state, which allows the DRO state to be left out of the NRHO filter state.

Each choice provides advantages and disadvantages. For Option (1), the main advantage is that the DRO orbit does not require ground-based tracking or OD solutions, but it is complicated by the addition of the DRO state to the NRHO filter. The addition of more filter states increases the computational requirements, and increases the sensitivity of the filter to tuning parameters. Also, given that the DRO orbit requires virtually no OMMs, having little to no ground based tracking reduces the operations cost for the DRO relay satellite.

For Option (2) the main advantage is that the DRO state can be left out of the NRHO filter state, creating a simpler processing and tuning scenario. However the primary disadvantage is this option creates a dependence on at least ground-based tracking, most likely including DSN tracking. For this reason Option (2) with a ground-based OD scenario is not considered in this analysis. The focus of this investigation is the feasibility of Option (1).

For the DSN-only cases, the SRIF state vector consists of the position, velocity and coefficient of reflectivity of the NRHO spacecraft. No additional measurement, environmental or acceleration biases are estimated. The SRIF state vector configuration for DRO-based navigation also includes the DRO relay's state. As with the DSN-solutions, no additional measurement, environmental or acceleration biases are estimated. In both the DRO and DSN solutions, the SRIF is allowed knowledge of the planned OMMs, but no other maneuver knowledge is included. The SRIF does not

estimate orbit maintenance maneuver corrections or attempt to model any of the disturbances of slews, deadbands or waste dumps. The filter configuration for both the DSN-base and DRO-based solutions is summarized in Table 3.

Table 3: SRIF State Vector Configurations

	DSN Tracking	DRO Tracking
NRHO State	Estimated	Estimated
NRHO C_r	Estimated	Estimated
DRO State	Not Estimated	Estimated
DRO C_r	Not Estimated	Estimated
Measurement Biases	Not Estimated	Not Estimated
Measurement Underweighting	Not Applied	Applied
Transponder Bias	Not Estimated	Not Estimated
Unmodeled Accelerations	Not Estimated	Not Estimated
Number of Estimated States	7	14

State And Filter Initialization

It is common practice in navigation analyses to test filter convergence by providing large a-priori state errors and commensurate covariances. However, a mission to an NRHO (crewed or otherwise) will not simply arrive at its destination orbit with little to no a-priori knowledge. The vehicle will be inserted from its out-bound Earth transfer orbit, complete with an OD state and covariance that has been carefully maintained along the way. Therefore, the filter states are initialized in the following way to approximate this injection condition. The filter is initialized with small a-priori errors and covariance and allowed to process data for half a revolution (approximately 3.25 days) before OMMs or disturbances are applied. The collection of solutions statistics begins at this point as well. The delayed start allows for a reasonable steady-state starting point for orbit maintenance planning.

Tracking Data

All four pairings of dynamical models and tracking scenarios (crewed/uncrewed and DRO/DSN) are examined under at least three different levels of tracking data: 8 hours every two days, 8 hours every day, and continuous tracking. Nominal pass lengths of less than 8 hours are not considered due to the reduced cost effectiveness of shorter passes from the DSN. The basic measurement types used are S-Band range and Doppler measurements for both relative and DSN tracking. The measurement statistics and error sources used for the data simulation are listed in Table 4. DSN tracking passes are generated according to the following rules:

- Passes are generated randomly within each station's visibility windows with a start epoch that allows for the required duration to be met.
- Passes of up to one hour less than the desired duration are also allowed if the nominal duration could not be met.
- The repetition of multiple subsequent passes from the same DSN station was not allowed.

The DRO tracking schedule generation is simpler; the spacecraft generates the requisite amount of data each day, and it remains quiet the remainder of the day. The timing of the passes is not randomized. The short, infrequent lunar blockages are ignored from a scheduling perspective; blockages are allowed to interrupt tracking if they occur during passes. Also, attitude and antenna slew rates are not considered. The two spacecraft are assumed to be able to communicate as long as there is line-of-sight visibility.

The relative tracking data from the DRO communications relay is initially generated to closely match the duration and frequency of the DSN tracking data (e.g. 8 hour passes each day). This approach maintains consistency between the tracking scenarios. However, it is certainly possible that for a specialized navigation architecture as proposed here, there will be greater flexibility of scheduling, allowing for more frequent and shorter tracking passes. Therefore, for the relative tracking cases, shorter, more frequent passes are considered that are equivalent to the total tracking of the DSN cases. For example, 8 hours of DSN tracking per day is compared to 4 hours every 1/2 day and 2 hours every 1/4 day. In this way the DRO-based solutions are investigated more completely.

Transponder delay errors for both data types are treated as small constant, corresponding to a bias that is estimated previously in the mission and then set to a constant value and removed from the estimation state. Each run is supplied a random error value as listed in Table 4. Additionally, for DSN tracking, the ionosphere is modeled with the International Reference Ionosphere (IRI) 2008 model. Ionospheric errors are applied as a random percent error that is re-sampled daily following the statistics in Table 4.

Table 4: Measurement Statistics and Error Sources

	DSN Tracking	DRO Tracking
Data Rate	60 s	60 s
Range Noise (1σ)	4.0 m	4.0 m
Range Bias (1σ)	0.5 m	0.0 m
Doppler Noise (1σ)	0.2 cm/s	0.2 cm/s
Doppler Bias (1σ)	0.0 cm/s	0.0 cm/s
Doppler Averaging Interval	10 s	10 s
Transponder Error (1σ)	$1.5e^{-12}$ s	$1.5e^{-12}$ s
Ionospheric Error (1σ)	7%	–

SIMULATION CONFIGURATION

The closed-loop maneuver planning and navigation simulation is modeled using FreeFlyer.[21] Each simulation case is run for 18 revolutions of the NRHO orbit, or about 120 days, corresponding to about 4 lunar orbits. This length of simulation is chosen to allow for modeling of two full cycles of the 9:2 resonance of the NRHO. After filtering for one half of a revolution to establish mostly steady-state behavior, statistics are collected to examine various aspects of the solutions. The maneuver planning quantities listed below are collected at every apoapsis, and additionally position and velocity errors and uncertanties are collected at every periapsis as well.

- NRHO Position / Velocity Error and 3σ uncertainty at maneuver planning time

- DRO Position / Velocity Error and 3σ uncertainty at maneuver planning time
- Planned Maneuver Magnitude
- Magnitude / Direction of Maneuver Planning Error
- Magnitude / Direction of Maneuver Execution Error
- NRHO Rotating Libration Point (RLP) Velocity Error

Maneuver execution errors are modeled as Gaussian random errors of 0.3% in magnitude and 0.3 degrees in direction (1σ, or 1% and 1 degree 3σ). The method by which maneuver planning errors are captured is relatively simple, given the benefit of a known truth state for the simulation. Each OMM is planned twice, once with the truth simulation state, and once with the navigation state. The difference between the two planned maneuvers is defined as the maneuver planning error.

For simulations of crewed conditions, orbit disturbances are applied over all 18 revolutions. This is longer than the expected duration of crewed visits to Gateway.[1] The added duration of crewed conditions allows for examination of filter stability over an extended time period. Keeping the crewed/uncrewed conditions in separate runs also eliminates the need to dynamically adjust the filter tuning in response to changing dynamical conditions. This simplification is useful in characterizing steady state performance differences between the filter configurations.

Filter Tuning

In general, the filter requires more process noise for crewed conditions, as can be expected. For the DSN processing, one value of process noise is sufficient for all tracking levels. For the DRO processing, lower tracking levels require more process noise than those with higher levels of tracking. More broadly, it can be said that the DRO-based filter is much more sensitive to tuning parameters than the DSN-based filter.

In the process of tuning the filter, it was also observed that the DRO-based navigation cases were more prone to divergence at lower tracking levels with crewed conditions. In contrast, neither DRO navigation with uncrewed conditions or DSN navigation (both crewed and uncrewed) do not diverge for any cases. In the crewed/DRO cases that initially diverged, it was observed that for some passes near periapsis, the first range measurement is accepted and the covariance is tightened to the point that the rest of the data is rejected. Figure 3 illustrates the one post-update residual in red and the pre-update residuals in blue, along with the $\pm 3\sigma$ expected residuals envelope. This constriction of the covariance results in as much as 30-40% of range measurements being rejected before the filter diverges completely, or eventually recovers. It was determined that this divergence was due to non-linear effects in the relative measurements paired with the larger covariances after prolonged filter propagation. The non-linear effects are also exacerbated by the filter's lack of knowledge of the dynamical disturbances, which creates an overly optimistic covariance.

In some cases of rejected range data, the filter is able to recover via processing of subsequent passes of Doppler data. The Doppler measurement processing eventually improve the solutions to the point that the range data would again be accepted. After that the filter eventually recovers to comparable steady-state performance, but there is typically a cost in increased maneuver planning error and ΔV costs. An example of this behavior appears in Figure 4. Five passes of range residuals

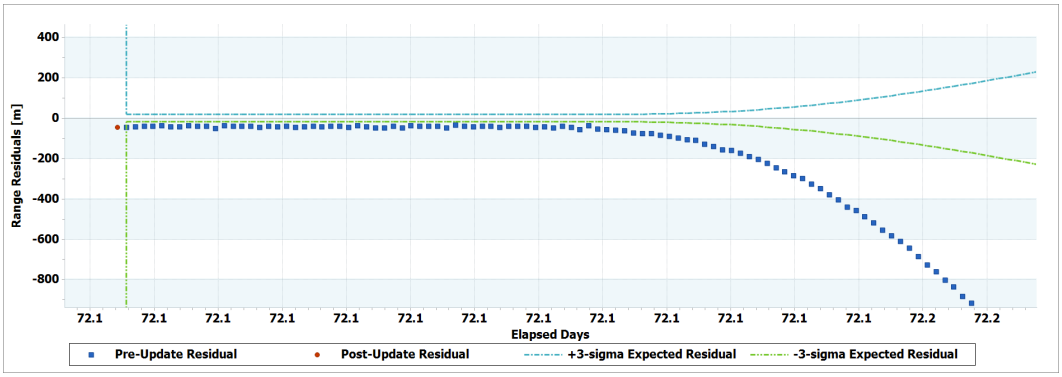

Figure 3: Pass Rejected Due to Non-linear Effects

are shown with the $\pm 3\sigma$ expected residuals envelope. Again, pre-update residuals are blue, and post-update are red. One entire pass of range (and Doppler) data is rejected, but on the subsequent pass, the Doppler data is accepted, which eventually brings the solution back to the point that the range data is accepted again.

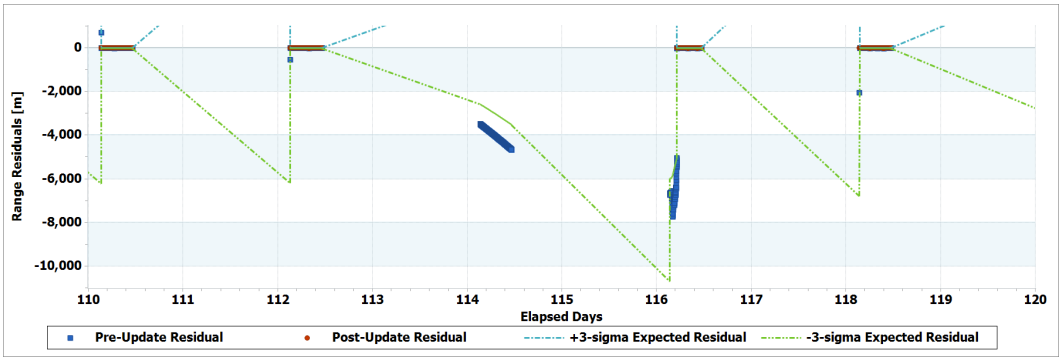

Figure 4: Solution Recovery after Processing Doppler Data

Therefore, prior to completing the analysis, the filter configuration was altered to include measurement underweighting in order to reduce the rate of covariance convergence at the beginning of each pass.[22] With the addition of underweighting and some process noise updates (as described previously), measurement acceptance is improved, and the overall rejection rate is reduced to the point of being comparable to the DSN cases (see Tables 7 and 8 included in the Results section).

However, these tuning changes were not able to prevent all measurement rejection at lower tracking levels. If the randomization of the orbit disturbances was applied in disadvantageous directions, the filter was still susceptible to rejection of range data while continuing to process Doppler data. This can also be seen in the difference in rejection rates in Tables 7 and 8, which are included in the Results section.

RESULTS

In all, 20 different combinations of tracking types, tracking levels, and dynamical conditions are considered. Forty different cases are run for each of these combinations, leading to a total of 800 cases run. Seven different tracking schedules are considered for DRO tracking, for both crewed

and uncrewed conditions. The DRO cases are compared to the 3 different tracking cases considered for the DSN according to cumulative tracking level over time. The complete breakdown of the combinations of tracking levels, data types, and dynamical conditions analyzed is listed in Table 5 with the number of cases run for each configuration.

Table 5: Summary of Cases Analyzed

	DRO Tracking		DSN Tracking	
Tracking Level	Uncrewed	Crewed	Uncrewed	Crewed
8 hrs / 2 d	40	40	40	40
4 hrs / 1 d	40	40	–	–
1 hrs / 0.25 d	40	40	–	–
8 hrs / 1 d	40	40	40	40
4 hrs / 0.5 d	40	40	–	–
2 hrs / 0.25 d	40	40	–	–
Continuous	40	40	40	40

Overall Filter Performance

In general, both filter solution types are able to produce viable OD solutions for use in conjunction with a receding-horizon maneuver planning process. One notable exception is the DRO navigation solution using the lowest level of tracking, 8 hours every 2 days, under crewed conditions. The filter diverged roughly 40% of the time. Because of this instability, the DRO results for crewed cases with low tracking levels are excluded from the reported results.

Prior to examining the summary statistics of all 800 runs, an example solution is shown in order to illustrate the broad characteristics that most solutions share. The representative cases shown are for 8 hours of tracking per day, corresponding to the intermediate tracking level. Figures 5(a) - 6(b) illustrate the total position errors and 3σ uncertainty for representative cases of DRO- and DSN-navigation during uncrewed and crewed periods. Figures 7(a) - 8(b) show the total velocity errors and 3σ uncertainty for the same four cases. In all figures, DRO solutions are on the left, and the DSN solutions are on the right. The NRHO errors and covariances are blue and red, respectively, and the DRO errors and covariances are teal and green, respectively. All plots use a logarithmic scale, with distance units in meters and velocities in cm/s.

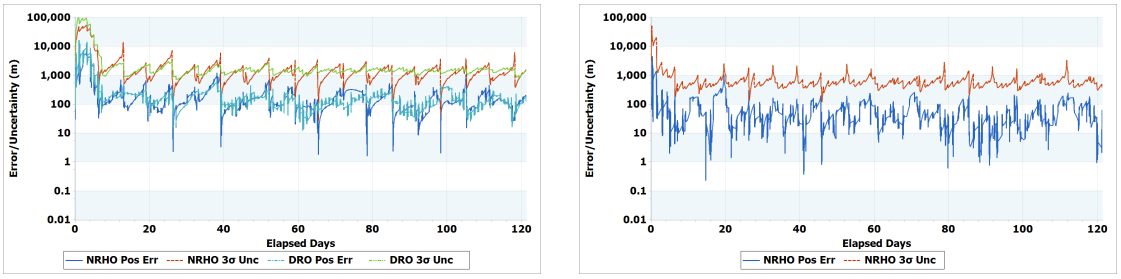

(a) Uncrewed DRO Navigation

(b) Uncrewed DSN Navigation

Figure 5: Representative Uncrewed Solution Position Characteristics

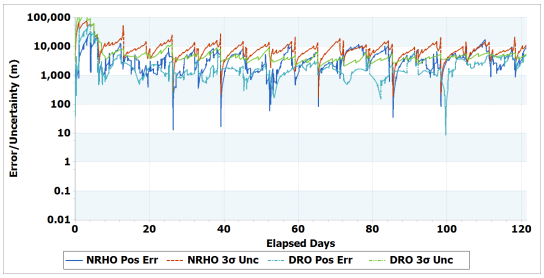

(a) Crewed DRO Navigation

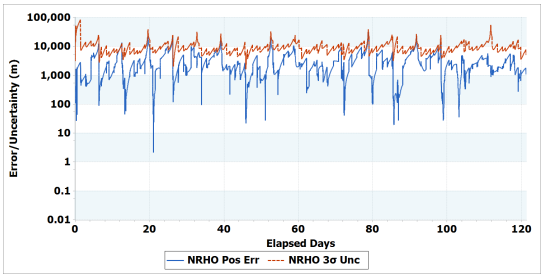

(b) Crewed DSN Navigation

Figure 6: Representative Crewed Solution Position Characteristics

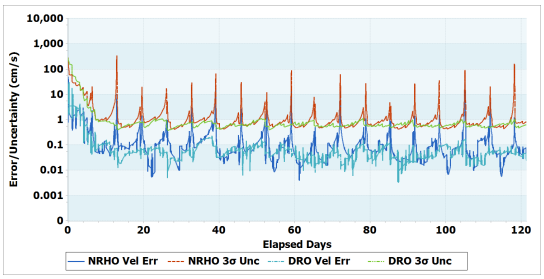

(a) Uncrewed DRO Navigation

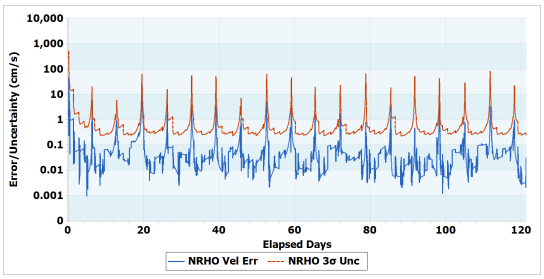

(b) Uncrewed DSN Navigation

Figure 7: Representative Uncrewed Solution Velocity Characteristics

Comparing the DRO- and DSN-based example solutions in Figures 5 - 8, it can can be seen that the DSN-based solutions generally provide only slightly better accuracy and less uncertainty at comparable tracking levels. This result is true for both crewed and uncrewed conditions; however the difference is more pronounced for uncrewed conditions. The addition of disturbances associated with crewed activity increases the position and velocity errors and uncertainty of both solution types. For all solution types, the errors and uncertainty trend lower around apoapsis, while the velocity errors and covariances spike around each periapsis passage.

All solution types also show a bit of re-convergence over the first orbit revolution once the maneuver planning process was initiated. This is seen in the downward trend of the errors and uncertainty

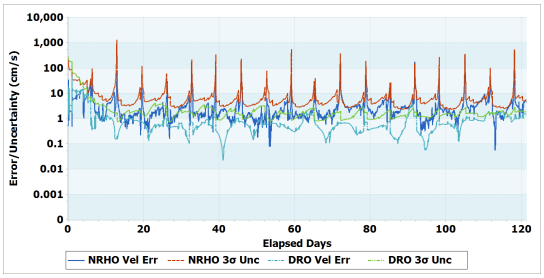

(a) Crewed DRO Navigation

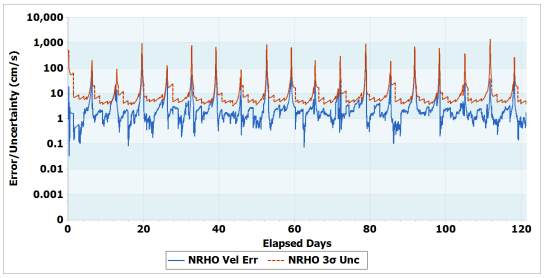

(b) Crewed DSN Navigation

Figure 8: Representative Crewed Solution Velocity Characteristics

over the first 10 days of the simulation. The convergence period is slightly shorter and less pronounced for the DSN cases; this is likely due to its simpler filter estimation state. The DRO filter is required to work out correlations between the NRHO and DRO states, which can prolong filter convergence. This increased convergence time for DRO solutions does produce a slight impact on maneuver planning performance, which is discussed later.

Table 6 provides a high-level summary of the overall performance of the 800 cases run. DRO tracking runs with the same overall tracking level are grouped in subsequent rows. Three quantities are shown for each of the 20 different configurations investigated. These include the average total ΔV and average 3σ position and velocity uncertainty at maneuver planning time (apoapsis). The total ΔV is the 40-case average of the sum of all OMMs for each run. The 3σ uncertainty averages are the average from all 720 maneuver planning opportunities (18 maneuvers x 40 runs). All distance units are meters, and all velocity units are cm/s.

Table 6: Summary of Average Filter Results over 18 Revolutions (m, cm/s)

		DRO Tracking			DSN Tracking		
	Tracking	Total ΔV	Position 3σ	Velocity 3σ	Total ΔV	Position 3σ	Velocity 3σ
Uncrewed	8 hrs / 2 d	143.41	1879.38	0.958	143.59	490.76	0.273
	4 hrs / 1 d	143.61	1465.46	0.743	—-	—-	—-
	1 hrs / 0.25 d	143.32	1350.41	0.688	—-	—-	—-
	8 hrs / 1 d	143.75	1595.17	0.823	143.47	392.51	0.230
	4 hrs / 0.5 d	143.45	1341.03	0.681	—-	—-	—-
	2 hrs / 0.25 d	143.53	1310.17	0.664	—-	—-	—-
	Continuous	143.37	1443.72	0.742	143.63	160.14	0.158
Crewed	8 hrs / 2 d	—-	—-	—-	152.23	8558.56	5.459
	4 hrs / 1 d	153.92	7513.15	3.521	—-	—-	—-
	1 hrs / 0.25 d	150.88	6409.38	3.111	—-	—-	—-
	8 hrs / 1 d	154.68	6972.75	3.318	144.32	6174.04	4.267
	4 hrs / 0.5 d	150.37	6440.10	3.124	—-	—-	—-
	2 hrs / 0.25 d	150.02	6306.91	3.070	—-	—-	—-
	Continuous	156.24	7718.68	4.606	144.42	774.07	2.152

By examining the averages of the uncrewed DRO and DSN solutions, several observations can be made. First, just as with the example plots, it can be seen that the DSN solutions provide tighter uncertainty at apoapsis than the DRO solutions. Secondly, the increased uncertainty of the DRO solutions does not translate to significantly higher orbit maintenance costs. This suggests that there is a base level of deterministic orbit maintenance costs for NRHOs, and uncertainty differences on the order of a few km does not have a significant impact on maintenance costs. Thirdly, for crewed conditions, the average OMM costs increase, but they increase more significantly for the DRO solutions than the DSN solutions. Overall, the uncertainties increase for all crewed solutions, but the level of increase is greater for the DSN cases, increasing from a few hundred meters in position to multiple kilometers.

The average values of velocity 3σ uncertainty as a function of overall tracking level appear in Figure 9. Each sub-plot shows both the crewed and uncrewed velocity uncertainties at both apoapsis and periapsis. The DSN solutions on the right show the four unique pairings of apoapsis/periapsis and crewed/uncrewed. The results are simple and clear: periapsis uncertainty is higher, and more

tracking reduces the uncertainty. Also, increasing the tracking level improves the periapsis uncertainty more than at apoapsis. This is likely a result of the elongation of the NRHO; the spacecraft spends more time near apoapsis. Tracking near apoapsis is virtually guaranteed at the levels studied here; increasing the tracking level increases the likelihood of good coverage of periapsis as well. These results apply to the DRO navigation solutions as well.

The sub-plot showing the DRO solution results is more complicated, and requires additional explanation. The same pairings as the DSN solutions are shown, but the additional cases of shorter, more frequent passes are also included. To limit the size of the legend, only the periapsis series names are included, and they are labeled by relative amount of time between passes (e.g. 1/2 for 4 hours every half day). Examination of the DRO solution covariances leads to multiple observations. First, increasing tracking levels has significantly more impact on periapsis uncertainty, and reduces them significantly, whereas at apoapsis the uncertainties are relatively unchanged. Secondly, the shorter more frequent passes also improve the uncertainties significantly, and the shortest, most frequent passes provide the greatest uncertainty reduction. Again, these effects are more pronounced at periapsis.

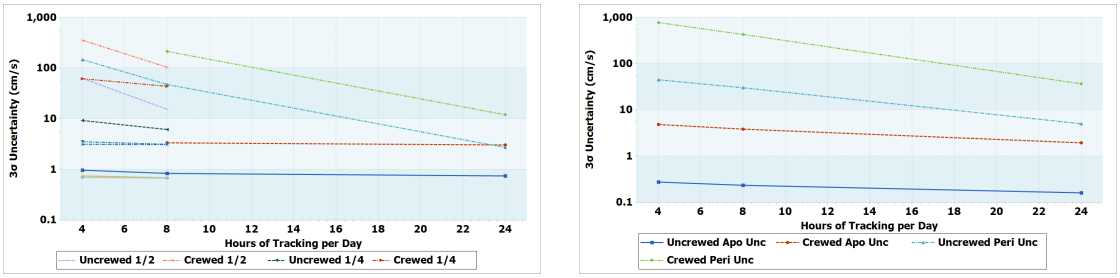

(a) DRO Navigation

(b) DSN Navigation

Figure 9: Apoapsis and Periapsis Velocity Covariance vs Tracking Level

One important difference between the DSN and DRO solutions is the uncertainty at periapsis under crewed conditions (the green line). The DRO-based velocity uncertainty at periapsis is actually less than the DSN-based uncertainty. This reduction in uncertainty is potentially a function of the differences in information content of the Doppler measurements. For the DSN solutions, the NRHO geometry is relatively fixed, with the majority of the spacecraft velocity perpendicular to the line-of-sight to the DSN stations. However, for the DRO / NRHO pairing, the geometry varies as the DRO orbits around the Moon. This geometry provides greater diversity of the Doppler measurement, with times when the NRHO velocity is mostly in the line-of-sight. These times correspond to when the NRHO is passing through periapsis and the DRO is at maximum RLP-Y amplitude. This diversity of Doppler data may explain why the DRO solutions are able to provide a more pronounced uncertainty reduction at periapsis.

Finally, some additional trends can be seen by comparing DRO cases where the tracking amount is constant, but the timing and duration of passes is changed (e.g. 8 hours per day vs. 4 hours every half day). Looking at the three cases with a total of 8 hours of tracking a day, it can be seen that the shorter, more frequent passes improves the position and velocity uncertainties, and helps to slightly reduce the OMM costs. However, the larger impact is on solution uncertainty at periapsis. The uncertainty reduction is significant, and impacts filter stability, as can be seen from the fact that no results are presented for the case of 8 hours of tracking every 2 days. The case of 4 hours of tracking

every day also achieves more stability with less time between passes.

Measurement Processing

Once the filter was tuned for processing during crewed conditions, it was able to achieve high levels of measurement acceptance, and post-update residual statistics that matched expected values. The uncrewed solutions produce very clean residual statistics. For brevity, only plots showing residuals for crewed conditions are included. Again, pre-update residuals are blue, and post update residuals are red. Figure 10 shows a representative case of both the DRO and DSN range residuals, and Figure 11 shows the Doppler residuals.

Again, DRO-based solutions are on the left, and DSN-based solutions are on the right. Overall the measurement statistics are comparable between the two tracking data types. It is clear from the plots that the post-update residuals are very nearly zero mean. However, the expected residuals for the DSN data show a variation that repeats 4 times over the course of the run. This pattern appears to be correlated to the lunar orbital period, as the Moon completes 4 revolutions over the length of the run. There are similar variations in the DRO Doppler data, associated with the NRHO orbital period; however these variations are very small and more difficult to discern.

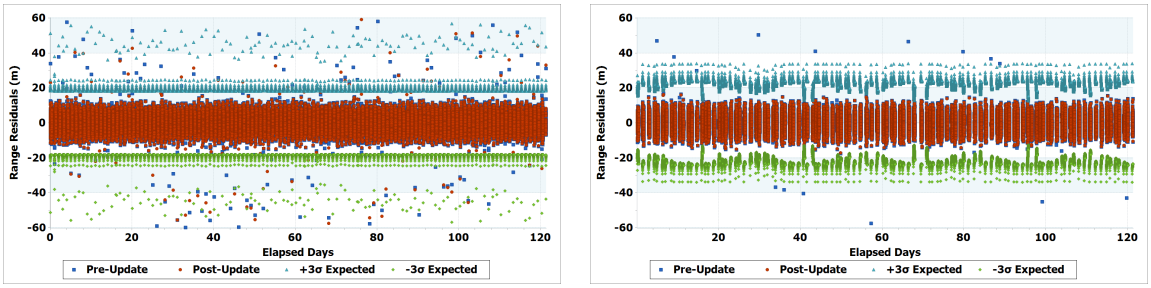

(a) Crewed DRO Navigation

(b) Crewed DSN Navigation

Figure 10: Pre- and Post-Update Range Residuals

One other item to note about the range residuals is that there are several measurements that were accepted by the filter, even though the post-update residual appears to be outside the typical Expected Residuals envelope. These points are simply measurements where measurement under-weighting is applied, so the state and covariance updates are scaled back from the nominal. In fact, for the range data, some underweighted residuals are actually beyond the scale of the plot. It is also important to note that these underweighted measurements are only present in the DRO-based range measurements. The DSN-tracking cases do not require underweighting, and the DRO-based Doppler requires underweighting for fewer measurements.

Tables 7 and 8 summarize the averaged range and Doppler statistics for all cases run. For all of the uncrewed cases, the range and Doppler statistics are exactly as one would expect from a well-performing filter. The mean values are all near zero, the RMS values are similar to the 1σ noise value, and there are very few rejected measurements. The DSN-tracking cases show the same behavior for crewed conditions; very clean, steady, robust filter performance.

However, for the DRO-tracking cases under crewed conditions, the statistics are a bit different. The mean values are also near zero, as with uncrewed cases. There are still relatively few rejected measurements, although there are slightly more than for uncrewed conditions. Again, this is to be

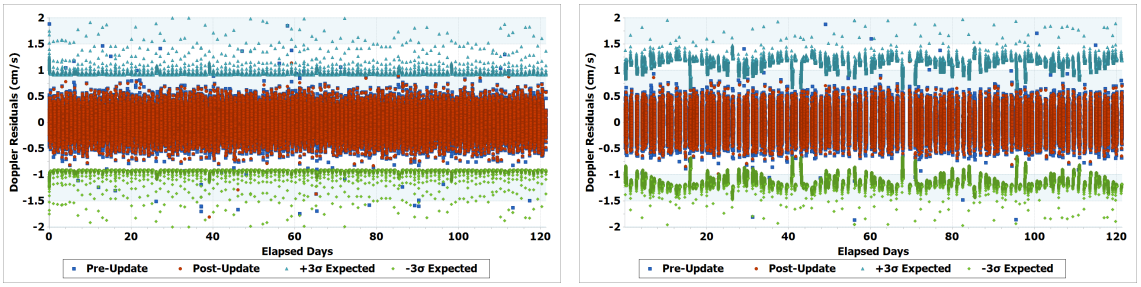

(a) Crewed DRO Navigation

(b) Crewed DSN Navigation

Figure 11: Pre- and Post-Update Doppler Residuals

expected. However, the RMS values of the range data are considerably higher than the expected 1σ noise value of 4 m. To a lesser extent this is true for the Doppler RMS values as well.

Table 7: Average Range Processing Statistics (m)

		DRO Tracking			DSN Tracking		
	Tracking	Mean	RMS	% Rejected	Mean	RMS	% Rejected
Uncrewed	8 hrs / 2 d	-0.005	3.888	0.02	0.003	3.936	0.01
	4 hrs / 1 d	0.004	3.872	0.02	—-	—-	—-
	1 hrs / 0.25 d	-0.001	3.872	0.01	—-	—-	—-
	8 hrs / 1 d	-0.003	3.888	0.02	0.002	3.950	0.029
	4 hrs / 0.5 d	0.001	3.950	0.02	—-	—-	—-
	2 hrs / 0.25 d	-0.005	3.913	0.01	—-	—-	—-
	Continuous	-0.001	3.901	0.01	0.005	3.962	0.005
Crewed	8 hrs / 2 d	—-	—-	—-	-0.015	3.923	0.01
	4 hrs / 1 d	-0.031	30.503*	1.28	—-	—-	—-
	1 hrs / 0.25 d	-0.017	7.542*	0.81	—-	—-	—-
	8 hrs / 1 d	-0.021	15.825*	0.80	0.001	3.926	0.27
	4 hrs / 0.5 d	-0.016	9.527*	0.80	—-	—-	—-
	2 hrs / 0.25 d	0.005	5.361*	0.58	—-	—-	—-
	Continuous	-0.004	3.970	0.16	0.001	3.933	0.01

* RMS values affected by measurement underweighting

The reason for the higher RMS values is the application of measurement underweighting. Measurement underweighting is applied for only the first few measurements of each pass. However, the state update reduction on the first measurement is significant enough to create (valid) post-update residuals on the order of hundreds of meters. Even though there are relatively few, their magnitude is enough to affect the RMS calculations. This was subsequently confirmed by making additional runs with underweighted measurements excluded from the statistics. For these cases, the range RMS values returned to the expected 1σ noise value.

One other thing to note is that the RMS values for the DRO/crewed cases can amount to a post-facto measure of how much the measurement underweighting is applied. The RMS values of the continuous tracking cases are close to the expected 1σ, meaning very few measurements are un-

Table 8: Average Doppler Processing Statistics (cm/s)

		DRO Tracking			DSN Tracking		
	Tracking	Mean	RMS	% Rejected	Mean	RMS	% Rejected
Uncrewed	8 hrs / 2 d	$3.7e^{-5}$	0.195	0.02	0.001	0.198	0.01
	4 hrs / 1 d	$-1.7e^{-4}$	0.195	0.02	—-	—-	—-
	1 hrs / 0.25 d	$4.2e^{-4}$	0.198	0.01	—-	—-	—-
	8 hrs / 1 d	$4.2e^{-5}$	0.195	0.01	0.001	0.199	0.01
	4 hrs / 0.5 d	$-1.9e^{-4}$	0.199	0.01	—-	—-	—-
	2 hrs / 0.25 d	$-2.0e^{-5}$	0.198	0.01	—-	—-	—-
	Continuous	$9.4e^{-5}$	0.195	0.01	-0.001	0.199	0.01
Crewed	8 hrs / 2 d	—-	—-	—-	-0.001	0.195	0.01
	4 hrs / 1 d	$5.2e^{-5}$	0.460*	0.80	—-	—-	—-
	1 hrs / 0.25 d	$-6.2e^{-4}$	0.243*	0.12	—-	—-	—-
	8 hrs / 1 d	$-3.5e^{-5}$	0.298*	0.41	0.001	0.19	0.05
	4 hrs / 0.5 d	$-2.1e^{-4}$	0.249*	0.29	—-	—-	—-
	2 hrs / 0.25 d	$2.8e^{-4}$	0.219*	0.06	—-	—-	—-
	Continuous	$-2.7e^{-4}$	0.206	0.01	-0.001	0.19	0.01

* RMS values affected by measurement underweighting

derweighted. As the propagation times increase and there is less data, the RMS values grow accordingly. The highest range RMS value corresponds to the case with the least amount of data and longest propagation between passes.

Maneuver Performance

The most significant impact of the crewed disturbances is to significantly increase the variance of the OMM costs. This is best illustrated in Figures 12(a) - 13(b). The figures show the OMM magnitudes for all 18 maneuvers in each of the 40 cases. The 40-case average is shown in each as the blue line, and the individual values are shown as points. By comparing the four plots, it can be seen that the average values for each OMM do not change much between DRO or DSN tracking and crewed or un-crewed conditions. However, there is a large difference in the variance of the OMM magnitudes, when comparing crewed and uncrewed conditions. The fact that the increased variability of the OMMs does not significantly change the average is likely a product of the randomized direction of the orbit disturbances. Improving the fidelity of modeling these disturbances will likely change these results, potentially increasing the average OMM costs.

Also, close examination of Figure 12(a) shows that OMM 1 and OMM 2 have a higher variance than the rest of the maneuvers in the DRO cases. The variance of these two is also higher than the variance of OMM 1 and 2 for the DSN case. This appears to be due to the fact that the DRO-based filter takes longer to converge than the DSN-based filter.

To better understand the specific relationship between the navigation error and maneuver planning error, the maneuver planning errors are collected and plotted as functions of various quantities at maneuver planning time. Of the quantities examined, a few have relationships of note. For example,

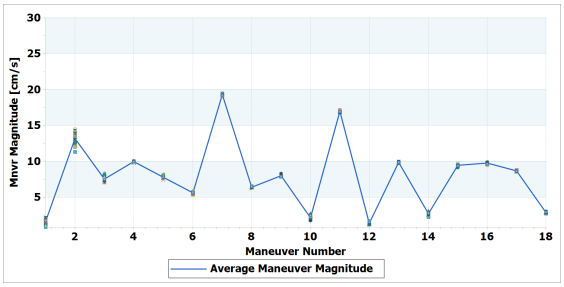

(a) Uncrewed DRO Navigation

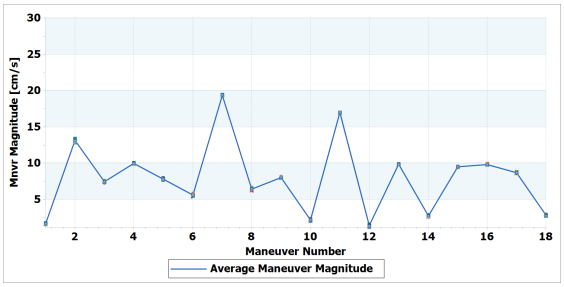

(b) Uncrewed DSN Navigation

Figure 12: Uncrewed Maneuver Magnitudes for 8 hours of Tracking per Day

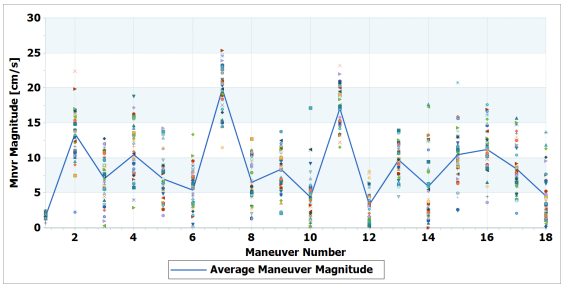

(a) Crewed DRO Navigation

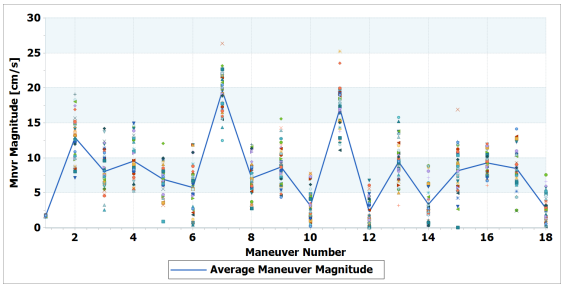

(b) Crewed DSN Navigation

Figure 13: CrewedManeuver Magnitudes for 8 hours of Tracking per Day

Figure 14 shows the maneuver planning error for all 720 maneuvers of the 40 DRO / DSN crewed / uncrewed cases run at 8 hours of tracking a day. Maneuver planning error is plotted as a function of the total velocity error at maneuver planning time. The DRO / Crewed combination is the noisiest data set, shown in blue, and the DSN / Uncrewed combination is the cleanest, shown in green.

It is clear from the plot that the maneuver planning error rarely exceeds the velocity error magnitude. The one-to-one ratio is plotted as the black diagonal line. It seems the velocity error essentially acts as a maximum value for the maneuver planning error. However, it can be seen that many points have larger velocity errors than total maneuver planning error. Given that the plot is is a function velocity error magnitude (and does not include direction information), these results seems to indicate that the direction of the velocity error has an impact on the resultant maneuver planning error.

As stated previously, the receding-horizon targeting approach attempts to match the magnitude of V_x in the RLP frame of the reference trajectory at periapsis 6.5 revolutions ahead. Given this dependence on RLP V_x, it is natural to look at the maneuver planning error as function of the error in V_x at maneuver planning time. This is illustrated in Figure 15. The colors of cases match those of Figure 14. Interestingly, there appears to be no significant correlation between the error in RLP V_x and maneuver planning error. The two crewed cases (blue and red) are noisy with no real pattern, and the two uncrewed cases (teal and green) show a wide range of RLP V_x errors, but consistently small maneuver planning errors.

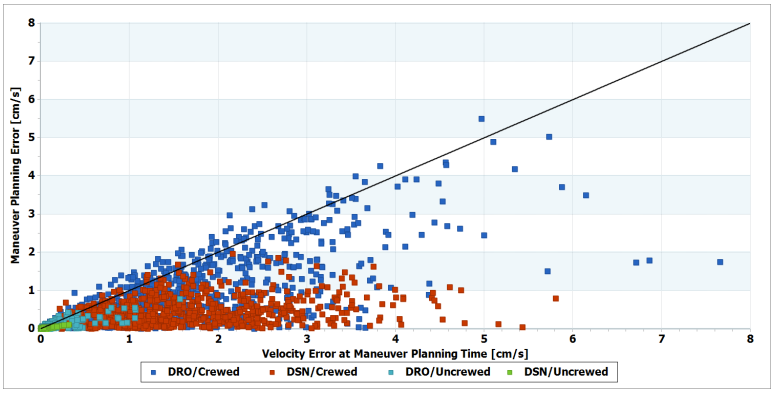

Figure 14: Maneuver Planning Error vs. NRHO Velocity Error Magnitude

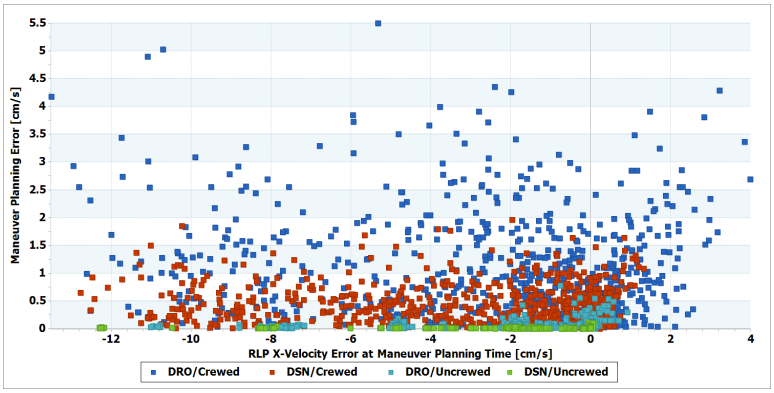

Figure 15: Maneuver Planning Error vs. NRHO RLP V_x Error

CONCLUSION

This analysis shows that relative-tracking strategies using a DRO are likely viable for spacecraft in an NRHO in some scenarios. In quiescent, uncrewed conditions, DRO-based tracking provided comparable ΔV costs for orbit maintenance, even with slightly higher orbit uncertainty, as compared to DSN-based tracking, across all tracking levels. In noisy, crewed conditions, the DSN-based solutions outperformed the DRO-based solutions, both in terms of orbit accuracy as well as ΔV costs for orbit maintenance. DRO-based solutions with tracking passes separated by more than 24 hours would likely not provide enough accuracy to maintian filter stability for the noisy environment associated with crewed conditions. DRO-based solutions with more frequent shorter passes performed better during crewed conditions.

For crewed conditions, all solutions suffered considerable variability in OMM costs, even though the mean values were relatively unchanged. The randomization of direction for all crewed disturbances appears to be the likely cause. Depending on the direction the disturbances are applied could lead to considerably higher or lower OMM costs. Furthermore, for the DRO cases, it can lead to rejection of valid range data. These results indicate that better modeling of the disturbances in the filter (or estimation of them) could improve performance for DRO-based navigation. The DSN-based solutions will benefit as well, but are overall much less sensitive in terms of measurement processing.

Furthermore, during crewed conditions, any DRO-based tracking strategy should account for non-linear effects in the measurements. These effects prove to be significant for cases with greater time between passes. Without underweighting in the filter, DRO-based solutions are prone to rejected passes and even divergence. Typically the filter rejects data from passes near periapsis. Sometimes the filter rejects the range data but accept the Doppler, allowing the filter to recover, but the consequence is increased OMM costs due to the increased orbit error.

This analysis does not consider explicit requirements on navigation accuracy, both definitive and predictive. This work instead focuses on how realistic navigation errors affect the receding-horizon maneuver planning approach being investigated for Gateway. This work shows DRO-based solutions as a feasible alternative, but the higher uncertainty may end up violating Gateway definitive or predictive accuracy requirements, depending on the specific values of those requirements.

Obviously, no human mission to the Moon would forgo DSN contacts entirely. The communications, telemetry, and mission safety requirements would likely necessitate at least some DSN contacts. Based on this analysis, DRO-based tracking would likely be sufficient for uncrewed conditions, or could be used to augment the DSN during crewed periods. If DSN contacts can be minimized during crewed phases and eliminated during uncrewed phases, the burden of cis-lunar missions on the DSN can be reduced through the addition of a tracking satellite in a DRO or potentially another cis-lunar orbit. Costs of such a relay mission will have to be weighed against the expected costs of DSN tracking for planned cis-lunar missions.

Future Work

There are several aspects of this work that warrant further investigation, either by adding greater fidelity to the current work, or addressing questions raised.

- Add greater fidelity to the dynamical disturbances of crewed phases, including attitude information, body-fixed disturbances, and representative crewed periods
- Add greater fidelity to the concept of operations for maneuver planning
- Consider a single filter configuration that incorporates both crewed and uncrewed conditions
- Consider range-only or Doppler-only solutions
- Consider other estimation methods, such as Batch Least Squares, or adding backward smoothing to the SRIF process
- Consider multiple relay spacecraft, phased around the DRO
- Examine dynamical models associated with various configurations of Gateway, at different phases of construction

ACKNOWLEDGMENTS

The authors would like to thank a.i. solutions and the Space Products Division for funding this research.

REFERENCES

[1] C. Newman, D. Davis, R. Whitley, J. Guinn, and M. Ryne, "Stationkeeping, Orbit Determination, and Attitude Control for Spacecraft in Near Rectilinear Halo Orbits," *AAS/AIAA Astrodynamics Specialists Conference*, Snowbird, UT, AAS/AIAA, August 2018.

[2] K. Hambelton, "Deep Space Gateway to Open Opportunities for Distant Destinations," Web, 3 2017. NASA.

[3] R. Whitley and R. Martinez, "Options for Staging Orbits in Cislunar Space," *2016 IEEE Aerospace Conference*, Big Sky, MT, IEEE, March 5-12 2016.

[4] D. Davis, S. Bhatt, K. Howell, J. W. Jang, R. Whitley, F. Clark, D. Guzzetti, E. Zimovan, and G. Barton, "Orbit Maintenance and Navigation of Human Spacecraft at Cislunar Near Rectilinear Halo Orbits," *AAS/AIAA Spaceflight Mechanics Meeting*, San Antonio, TX, AAS/AIAA, February 5-9 2017. AAS 17-269.

[5] D. Guzzetti, E. Zimovan, D. Davis, and K. Howell, "Stationkeeping Analysis for Spacecraft in Lunar Near Rectilinear Halo Orbits," *AAS/AIAA Spaceflight Mechanics Meeting*, San Antonio, TX, AAS/AIAA, February 5-9 2017. AAS 17-395.

[6] J. Crusan, "Future Human Exploration Planning: Lunar Orbital Platform - Gateway and Science Workshop Findings," NASA.gov, March 207 2018. https://www.nasa.gov/sites/default/files/atoms/files/20180327-crusan-nac-heoc-v8.pdf.

[7] Wikipedia. Web, June 2018. https://en.wikipedia.org/wiki/Lunar_Orbital_Platform-Gateway#Proposed_timeline.

[8] C. Shouraboura, M. D. Johnston, and D. Tran, "Prioritization and Oversubscribed Scheduling for NASA's Deep Space Network," *Workshop on Scheduling and Planning Applications, International Conference on Automated Planning and Scheduling (SPARK, ICAPS 2016)*, London, UK, June 2016.

[9] L. David, "Mars' Looming Traffic Jam," *Space News Magazine*, April 24, 2017.

[10] NASA, "NASA's Mission Operations and Communications Services," October 1, 2014. https://deepspace.jpl.nasa.gov/files/6_NASA_MOCS_2014_10_01_14.pdf.

[11] K. Hill, G. Born, and M. Lo, "Linked, Autonomous, Interplanetary Satellite Orbit Navigation (LiAISON) in Lunar Halo Orbits," *AIAA/AAS Astrodynamics Specialist Conference*, Lake Tahoe, CA, AAS/AIAA, August 7-11 2005. AAS 05-400.

[12] K. Hill, J. Parker, G. Born, and N. Demandante, "A Lunar L2 Navigation, Communication, and Gravity Mission," *AIAA/AAS Astrodynamics Specialist Conference*, Keystone, CO, AAS/AIAA, August 21-24 2006. AIAA 2006-6662.

[13] P. Liu, X. Hou, J. S. Tang, and L. Liu, "Application of two special oribts in the orbit determination of Lunar satellites," *Research in Astronomy and Astrophysics*, Vol. 14, No. 10, 2014, pp. 1307–1328.

[14] I. Murphy, "Advanced Space Wins $ 250,000 Innovation Award from Colorado Office of Economic Development and International Trade," Business Wire, June 2017. https://www.businesswire.com/news/home/20180607005363/en/Advanced-Space-Wins-250000-Innovation-Award-Colorado.

[15] C. Bezrouk and J. Parker, "Long Duration Stability of Distant Retrograde Orbits," *AIAA/AAS Astrodynamics Specialist Conference*, San Diego, CA, AAS/AIAA, August 4-7 2014. AIAA 2014-4424.

[16] G. Turner, "Results of Long-Duration Simulation of Distant Retrograde Orbits," *Aerospace*, Vol. 3, No. 4, 2016.

[17] G. Wawrzyniak and K. Howell, "An Adaptive, Receding-Horizon Guidance Strategy for Solar Sail Trajectories," *AIAA/AAS Astrodynamics Specialist Conference*, Minneapolis, MN, AAS/AIAA, August 13-16 2012. AIAA 2012-4434.

[18] G. Born, B. Schutz, and B. Tapley, *Statistical Orbit Determination*. Elsevier, 1st ed., May 2004.

[19] C. D'Souza, "On the Square Root Information Filter and Square Root Information Smoother Forumulation," *NASA EG Technical Brief*, No. FltDyn-CEV-16-X, 2016.

[20] C. D'Souza and G. Barton, "Process Noise Assumptions for Orion Cislunar Missions," *NASA MPCV Technical Brief*, No. FltDyn-CEV-16-50, August 2016.

[21] FreeFlyer. Mission Version 7.3.1, 2018. https://ai-solutions.com/freeflyer/.

[22] R. Zanetti, K. DeMars, and R. Bishop, "Underweighting Nonlinear Measurements," *Journal of Guidance Control and Dynamics*, Vol. 33, 09 2010, pp. 1670–1675.